J|A|C|S
ARTICLES
Published on Web 07/19/2006

A Simple γ-Backbone Modification Preorganizes Peptide Nucleic Acid into a Helical Structure

Anca Dragulescu-Andrasi, Srinivas Rapireddy, Brian M. Frezza,[†] Chakicherla Gayathri, Roberto R. Gil,* and Danith H. Ly*

Contribution from the Department of Chemistry, Carnegie Mellon University, 4400 Fifth Avenue, Pittsburgh, Pennsylvania 15213

Received April 12, 2006; E-mail: dly@andrew.cmu.edu; rgil@andrew.cmu.edu

Abstract: Peptide nucleic acid (PNA) is a synthetic analogue of DNA and RNA, developed more than a decade ago in which the naturally occurring sugar phosphate backbone has been replaced by the *N*-(*2*-aminoethyl) glycine units. Unlike DNA or RNA in the unhybridized state (single strand) which can adopt a helical structure through base-stacking, although highly flexible, PNA does not have a well-defined conformational folding in solution. Herein, we show that a simple backbone modification at the γ-position of the *N*-(2-aminoethyl) glycine unit can transform a randomly folded PNA into a helical structure. Spectroscopic studies showed that helical induction occurs in the C- to N-terminal direction and is sterically driven. This finding has important implication not only on the future design of nucleic acid mimics but also on the design of novel materials, where molecular organization and efficient electronic coupling are desired.

Introduction

Biotechnology applications, for the most part, are developed on the basis of the ability of specific substrates to bind to cellular targets. Such binding would either interfere with the physiological function of the targets and/or elicit the reporter signals. Establishing high binding affinity and selectivity between the substrates and the targets is crucial to the success of many of these applications. One way to achieve this goal would be to preorganize the substrates into the binding conformation prior to complexation. This would minimize the entropic penalty associated with most molecular recognition events and increase the rigidity of the substrates—thereby providing both stability and selectivity.[1] While this concept has been successfully applied to the design of small molecules for guest−host recognition,[2] it has been less successful with the design of larger and more flexible oligomeric molecules such as peptides and nucleic acids and their synthetic mimics, due to the large degree of freedom—although some progress has been made.[3−9] In this article we show that a simple γ-backbone modification can transform a randomly folded peptide nucleic acid (PNA) into a right-handed helix. These conformationally preorganized helical PNAs bind to DNA and RNA with exceptionally high affinity and sequence selectivity.

PNA is a synthetic analogue of DNA and RNA, developed more than a decade ago, in which the naturally occurring sugar phosphate backbone has been replaced by the *N*-(2-aminoethyl) glycine units, Scheme 1.[10] PNA can hybridize to complementary DNA or RNA strand through Watson−Crick base-pairing; because of the unnatural backbone, PNA can neither be recognized nor easily degraded by proteases or nucleases—all of which make PNA an attractive reagent for biotechnology applications.[11] However, unlike DNA or RNA in the unhybridized state (single strand) whose structure, to a large degree, is extended in solution due to the negatively charged phosphate backbone, PNA tends to fold into complex globular structures,[12,13] presumably due to the collapse of the hydrophobic nucleobases. In fact, this conformational collapse has been exploited in the development of stemless PNA molecular beacons, taking advantage of the proximity between the two termini in the unhybridized state.[12,14−16] Several modifications have been made to the PNA *N*-(2-aminoethyl) glycine backbone in attempts to increase its rigidity;[17,18] however, only a few such modifications showed improvements in the hybridization properties[19−24]—many of which require either elaborate

[†] Present address: The Scripps Research Institute, 10550 North Torrey Pines Road, La Jolla, CA 92037.

(1) Cram, D. J. *CHEMTECH* **1987**, *17*, 120−125.
(2) Cram, D. J. *Science* **1988**, *240*, 760−767.
(3) Kool, E. T. *Chem. Rev.* **1997**, *97*, 1473−1487.
(4) Gellman, S. H. *Acc. Chem. Res.* **1998**, *31*, 173−180.
(5) Cheng, R. P.; Gellman, S. H.; DeGrado, W. F. *Chem. Rev.* **2001**, *101*, 3219−3232.
(6) Dervan, P. B.; Edelson, B. S. *Curr. Opin. Struct. Biol.* **2003**, *13*, 284−299.
(7) Barron, A. E.; Zuckermann, R. N. *Curr. Opin. Chem. Biol.* **1999**, *3*, 681−687.
(8) Zondlo, N. J.; Schepartz, A. *J. Am. Chem. Soc.* **1999**, *121*, 6938−6939.
(9) Wengel, J. *Acc. Chem. Res.* **1999**, *32*, 301−310.
(10) Nielsen, P. E.; Egholm, M.; Berg, R. H.; Buchardt, O. *Science* **1991**, *254*, 1497−1500.
(11) Nielsen, P. E. *Acc. Chem. Res.* **1999**, *32*, 624−630.
(12) Gildea, B. D.; Coull, J. M.; Hyldig-Nielsen, J. J.; Fiandaca, M. J. WO A-9921881, 1999.
(13) Tackett, A. J.; Corey, D. R.; Raney, K. D. *Nucleic Acids Res.* **2002**, *30*, 950−957.
(14) Seitz, O. *Angew. Chem., Int. Ed.* **2000**, *39*, 3249−3252.
(15) Ranasinghe, R. T.; Brown, L. J.; Brown, T. *Chem. Commun.* **2001**, 1480−1481.
(16) Kuhn, H.; Demidov, V. V.; Coull, J. M.; Fiandaca, M. J.; Gildea, B. D.; Frank-Kameneteskii, M. D. *J. Am. Chem. Soc.* **2002**, *124*, 1097−1103.
(17) Beck, F.; Nielsen, P. E. *Artificial DNA: methods and applications*; CRC Press: Boca Raton, 2003.
(18) Kumar, V. A.; Ganesh, K. N. *Acc. Chem. Res.* **2005**, *38*, 404−412.
(19) Pokorski, J. K.; Witschi, M. A.; Purnell, B. L.; Appella, D. H. *J. Am. Chem. Soc.* **2004**, *126*, 15067−15073.

10.1021/ja0625576 CCC: $33.50 © 2006 American Chemical Society

Scheme 1. Chemical Structure of DNA (RNA), PNA and L-serine Derived γPNA (^{L}S-γPNA)

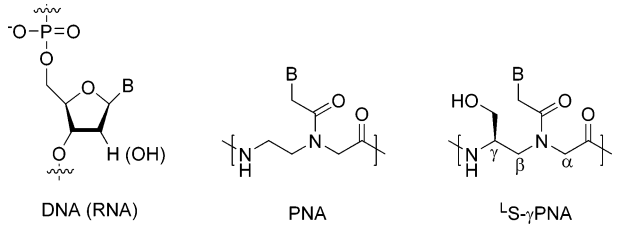

synthesis[19−22] or the use of relatively expensive D-amino acids as starting materials.[23,24] Of the various backbone modifications that have been made, only a few were made at the γ-position.[25−27] A systematic study correlating structure with function at this position has not yet been established. To fill this void, we have developed a research program to explore the structural effects of γ-backbone modifications on the conformation and hybridization properties of PNA.

Results and Discussion

Rationale. We decided to incorporate L-serine side chain at the γ-position of the PNA backbone because MD simulations showed that this configuration is less disruptive to hybridization than the D-configuration, and we reasoned that, since the serine side chains (OH groups) can form hydrogen bonds (H-bond) with water molecules, their inclusion could enhance the solubility of PNA in aqueous solution. PNA monomers and oligomers containing L-serine side chains at the γ-position (^{L}S-γPNAs) were synthesized (Scheme S1, Figures S1 and S2: Supporting Information), and their conformation and hybridization properties were characterized by CD, UV−vis, and multidimensional NMR spectroscopy. The sequence shown in P1−P5 (Figure 1) was chosen for this study because the hybridization properties of this particular PNA (P1) oligomer have been well-characterized.[28]

The Effects of γ-Backbone Modification on the Conformation of PNA. A comparison of the CD spectra of PNA (P1) and ^{L}S-γPNAs (P2−P5) is shown in Figure 1. No exciton coupling pattern was observed for P1 in the nucleobase absorption regions (220−300 nm). This generally indicates the lack of either helical base-stacking or excess helical sense (an equal mixture of right-handed and left-handed helical structures)—neither of which induces CD signal in this region. Although possible,[29] the second scenario is unlikely based on experimental findings.[30] On the other hand, we noticed distinct CD signals for P2−P5, with biphasic exciton coupling patterns characteristic

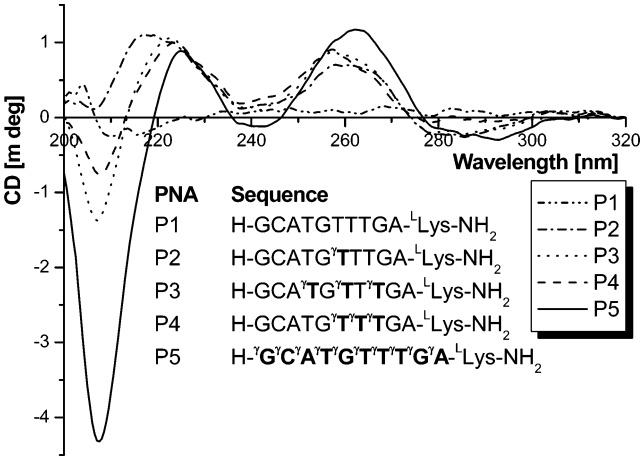

Figure 1. CD spectra of single-stranded PNA (P1) and ^{L}S-γPNAs (P2−P5). Bold letters denote the ^{L}S-γPNA units shown in Scheme 1. All samples were prepared in sodium phosphate buffer (10 mM sodium phosphate, 100 mM NaCl, 0.1 mM EDTA) at 2 μM strand concentration each. The CD spectra were recorded at 22 ° C unless otherwise stated.

of right-handed helices.[31] The CD profiles gradually shifted with increasing number of modified backbone units, from ones that resemble right-handed PNA−PNAs[30] to ones that resemble PNA−DNA helices[32]—as characterized by the negative band at the 240 nm and a red-shift in the 215 nm maximum. The most significant changes occurred in the 200−230 nm regions, with a dramatic increase in the amplitude of the 210 nm band. This spectral region has been previously assigned to the n−π* transition of the amides in the backbone.[33] The shift in the spectrum could be attributed to the variation in the backbone conformation, reflecting the helical twist of the oligomers. As the number of modified backbone units increases, the helical twist of the oligomer as a whole becomes more pronounced.

The Effects of Temperature and Concentration on the Exciton Coupling Patterns. To ensure that the observed exciton coupling occurs as the result of molecular preorganization (not intermolecular interaction), we performed temperature- and concentration-dependent CD measurements on P5. Our results showed that the intensities of the CD signals gradually decreased with increasing temperature, Figure 2. The exciton coupling pattern disappeared at around 60 °C—at which point the CD profile of P5 resembles that of P1 recorded at 22 °C. However, upon cooling, the CD signal returned to the original state, indicating that the observed exciton coupling is the intrinsic property of P5 and not the result of some artifact. We ruled out the possibility of intermolecular interaction, since the concentration-dependent study showed that the amplitude of the CD signals increased linearly with increasing concentration over a 100-fold range, Figure 3. Helical induction, inferred from the exciton coupling patterns, appears to be general to all serine-derived γPNAs since similar CD spectra were observed for other oligomers with different nucleobase sequence composition (Figure S3: Supporting Information).

The Effects of α- and γ-Backbone Modification on the Conformation of PNA. This is not the first time that exciton

(20) Lagriffoule, P.; Wittung, P.; Eriksson, M.; Jensen, K. K.; Norden, B.; Buchardt, O.; Nielsen, P. E. *Chem. Eur. J.* **1997**, *3*, 912−919.
(21) Dueholm, K. L.; Petersen, K. H.; Jensen, D. K.; Egholm, M.; Nielsen, P. E.; Buchardt, O. In *Bioorg. Med. Chem. Lett.* **1994**, *4*, 1077−1080.
(22) Govindaraju, T.; Kumar, V. A.; Ganesh, K. N. *J. Am. Chem. Soc.* **2005**, *127*, 4144−4145.
(23) Haaima, G.; Lohse, A.; Buchardt, O.; Nielsen, P. E. *Angew. Chem., Int. Ed. Engl.* **1996**, *35*, 1939−1942.
(24) Sforza, S.; Corradini, R.; Ghirardi, S.; Dossena, A.; Marchelli, R. *Eur. J. Org. Chem.* **2000**, 2905−2913.
(25) Englund, E. A.; Appella, D. H. *Org. Lett.* **2005**, *7*, 3465−3467.
(26) Tedeschi, T.; Sforza, S.; Corradini, R.; Marchelli, R. *Tetrahedron Lett.* **2005**, *46*, 8395−8399.
(27) Dose, C.; Seitz, O. *Org. Lett.* **2005**, *7*, 4365−4368.
(28) Demidov, V. V.; Protozanova, E.; Izvolsky, K. I.; Price, C.; Nielsen, P. E.; Frank-Kamenetskii, M. D. *Proc. Natl. Acad. Sci. U.S.A.* **2002**, *99*, 5953−5958.
(29) Sen, S.; Nilsson, L. *J. Am. Chem. Soc.* **2001**, *123*, 7414−7422.
(30) Wittung, P.; Nielsen, P. E.; Buchardt, O.; Egholm, M.; Norden, B. *Nature* **1994**, *368*, 561−563.
(31) Johnson, W. C. In *Circular Dichroism: Principles and Applications*; Wiley-VCH: New York, 2000.
(32) Egholm, M.; Buchardt, O.; Christensen, L.; Behrens, C.; Freier, S. M.; Driver, D. A.; Berg, R. H.; Kim, S. K.; Norden, B.; Nielsen, P. E. *Nature* **1993**, *365*, 566−568.
(33) Nielsen, E. B.; Schellman, J. A. *J. Phys. Chem.* **1967**, *71*, 2297−2304.

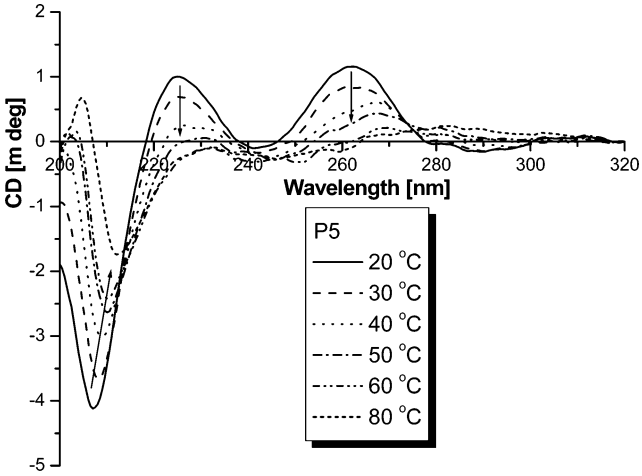

Figure 2. Temperature-dependent CD profiles of ^{L}S-γPNA (P5) at 2 μM strand concentration, prepared in sodium phosphate buffer. Arrows show the direction of increasing temperature.

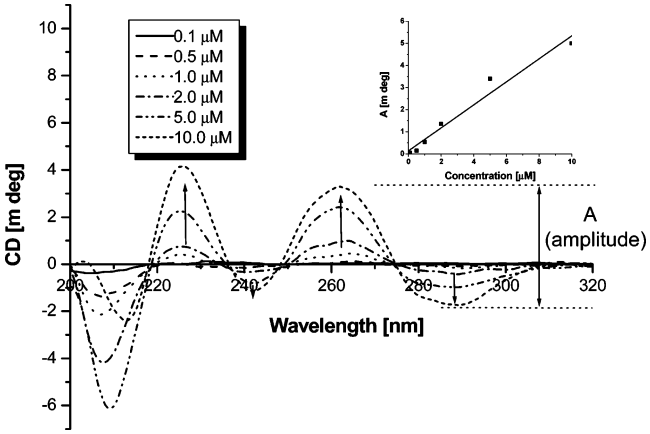

Figure 3. CD spectra of P5 oligomer at various concentrations. The samples were prepared in sodium phosphate buffer and recorded at 22 °C. (Inset) Plot of CD amplitude (A) vs P5 concentration.

coupling between neighboring nucleobases has been observed with chiral PNAs. Sforza and co-workers[34] showed that PNAs containing α-backbone modifications exhibited distinct CD patterns with the characteristic profile of a PNA−PNA double helix. However, it should be noted that the CD signals of these α-PNAs are weak compared to those of ^{L}S-γPNAs. A direct comparison can be seen in Figure 4, which shows that PNA containing L-serine side chain at the α-position (P6) did not show exciton coupling at 5 μM concentration as compared to PNA with the same side chain placed at the γ-position (P7), which showed pronounced Cotton effects characteristic of a right-handed PNA−DNA helix. The fact that the CD profile of P7, which contains one chiral unit, and that of P8, which contains four chiral units, are similar to one another, in both shape and amplitude in the nucleobase absorption regions, suggests that a single chiral unit may be sufficient to preorganize the entire oligomer into a helical structure—akin to the "sergeants and soldiers" concept developed by Green and co-workers[35] to explain the effects of chiral induction in polymers.

(34) Sforza, S.; Haaima, G.; Marchelli, R.; Nielsen, P. E. *Eur. J. Org. Chem.* **1999**, *197*, 7−204.
(35) Green, M. M.; Cheon, K.-S.; Yang, S.-Y.; Park, J.-W.; Swansburg, S.; Liu, W. *Acc. Chem. Res.* **2001**, *34*, 672−680.

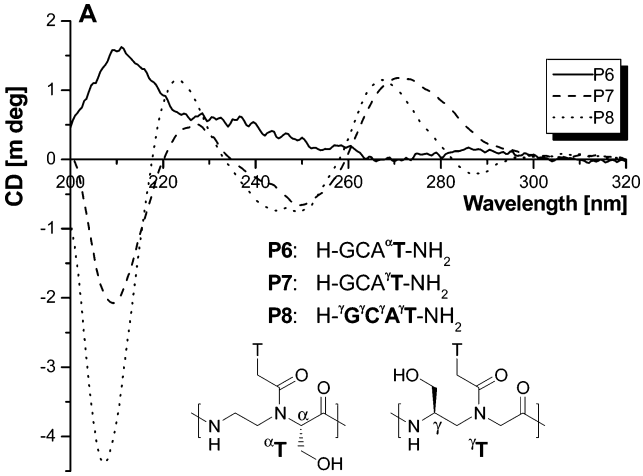

Figure 4. CD spectra of PNA containing α- and γ-backbone modifications. This particular oligomer, which comprised all four nucleobases, was chosen for this study as a model system because of the simplicity in the synthesis. The concentration of each strand was 5 μM in sodium phosphate buffer; CD spectra were recorded at 22 °C.

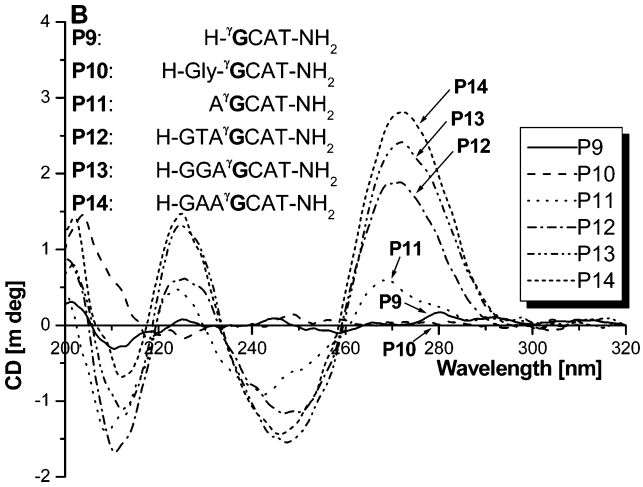

Figure 5. Spectroscopic evidence showing that helical induction occurs in the C- to N-terminal direction. The concentration of each strand was 15 μM in sodium phosphate buffer; CD spectra were recorded at 22 °C.

The Effects of γ-Backbone Modification on the Directionality of Helical Induction. Interestingly, we noticed the absence of CD signals when the chiral unit was switched from the C to the N terminus (compare the CD profile of P9 in Figure 5 to that of P6 in Figure 4). Notice that the concentration of P9 in Figure 5 is 3 times higher than that of P6 in Figure 4, but still no CD signal was observed for P9. Addition of an abasic glycine unit (P10) had no effect on the CD profile (still no CD signals). However, to our surprise we noticed that the CD signal characteristic of a right-handed PNA−DNA helix reappeared upon addition of an achiral PNA unit containing adenine nucleobase (P11). The amplitude of the CD signal further increased with additional achiral PNA units (compare the CD profiles of P12, P13, and P14 to that of P11 and P9). The difference in the signal intensities of P12, P13, and P14 at the 260−290 nm regions could be attributed to the difference in the extinction coefficient of the nucleobases, since different nucleobases were added to each oligomer. Together these results suggest that helical induction is unidirectional, occurring in the C to N terminus. Helical induction, however, does not appear

Scheme 2. Chemical Structure[a] of a Model (CT) PNA, L-Serine-Derived (LSer-γPNA) and L-Alanine-Derived (LAla-γPNA) γPNA System

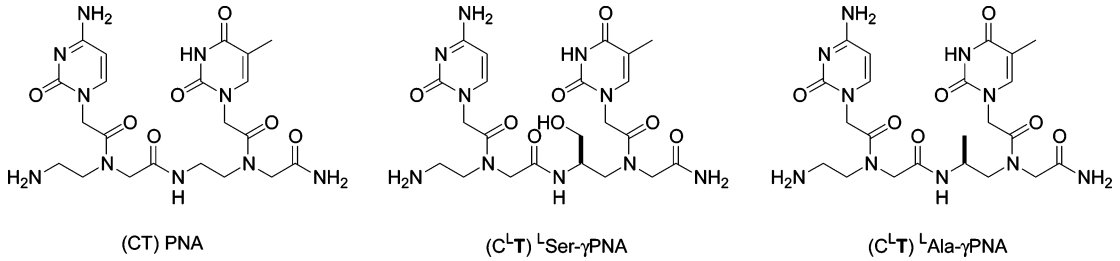

[a] The sequence is written from N to C terminus.

Scheme 3. Chemical Structures of the Four (CT) PNA Rotamers

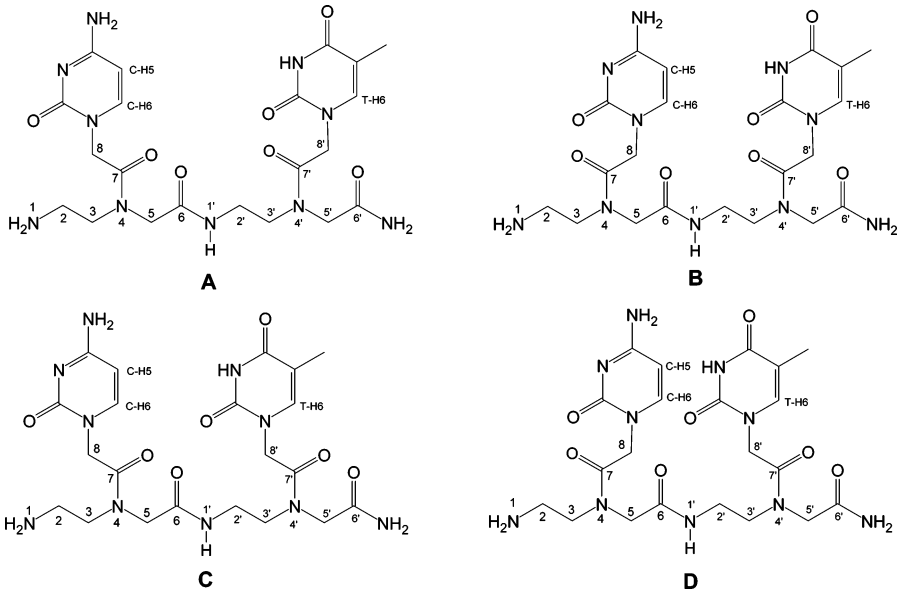

to be specific to the serine side chain since other amino acid side chains incorporated at the γ-position, including cysteine and alanine, showed similar exciton coupling patterns (data not shown).

Solution Structure of a Model System. To gain further insight into the conformation of γPNAs, we performed a series of multinuclear and multidimensional NMR experiments on a model (CT) PNA, L-serine-derived (LSer-γPNA) and L-alanine-derived (LAla-γPNA)[36] γPNA system (Scheme 2) using a Bruker Avance DMX-500 instrument operating at 500.13 MHz for ^{1}H and 125.77 MHz for ^{13}C. However, only PNA and LAla-γPNA dimers were examined in detail because LSer-γPNA showed extensive signal overlap and many of the characteristic spectral features observed in LSer-γPNA were also observed in LAla-γPNA, indicating similar conformational folding between the two systems. The data were collected on samples dissolved in D_2O. The full NMR assignments were performed using the following experiments: 1-D ^{1}H NMR, ^{1}H,^{1}H correlation spectroscopy (COSY), ^{1}H,^{1}H nuclear Overhauser spectroscopy (NOESY), ^{1}H,^{13}C heteronuclear single-quantum correlation spectroscopy (HSQC), and ^{1}H,^{13}C selective heteronuclear multiple bond correlation spectroscopy (SHMBC).

Solution Structure of (CT) PNA Dimer. It is well-known that the restricted rotation around the tertiary amide bond in PNA produces two possible rotamers in solution around the C7−N4 bond (tertiary amide bond), Scheme 3.[37−39] This characteristic of PNA monomers leads to signal duplication in the ^{1}H NMR spectrum. The NMR spectrum gets more complicated as the number of monomeric units increases because the number of rotamers in solution is equal to 2^n, where n is the number of monomeric units in the PNA strand. For a dimer, $2^2 = 4$ possible rotamers are expected to be present in solution. Scheme 3 shows the four possible rotamers for the (CT) PNA dimer. In fact, this is what was observed in the ^{1}H NMR spectrum. The spectrum showed four sets of signals with different intensities, corresponding to the aromatic protons in the bases C−H5, C−H6, TCH_3, and T−H6 (Figure 6, insets A−D). To complete the NMR assignment, the following strategy was used. The cytosine and thymine H-6 aromatic protons in each rotamer were used as the starting points, NOE cross-peaks in the NOESY spectrum led to signals corresponding to the methylene protons H-8 and H-8′. These signals in turn, led to another set of signals corresponding to H-5 and H-5′ via a common long-range proton−carbon correlation with the carbonyl carbon C-7 and C-7′ in the HMBC spectrum, respectively. This correlation is always present regardless of the geometry of the C7−N4 bond. To determine the geometry of the tertiary amide bond, the

(36) Kosynkina, L.; Wang, W.; Liang, T. C. *Tetrahedron Lett.* **1994**, *35*, 5173−5176.

(37) Dueholm, K. L.; Egholm, M.; Behrens, C.; Christensen, L.; Hansen, H. F.; Vulpius, T.; Petersen, K. H.; Berg, R. H.; Nielsen, P. E.; Buchardt, O. *J. Org. Chem.* **1994**, *59*, 5767−5773.

(38) Krotz, A. H.; Buchardt, O.; Nielsen, P. E. *Tetrahedron Lett.* **1995**, *36*, 6937−6940.

(39) Chen, S. M.; Mohan, V.; Kiely, J. S.; Griffith, M. C.; Griffey, R. H. *Tetrahedron Lett.* **1994**, *35*, 5105−5108.

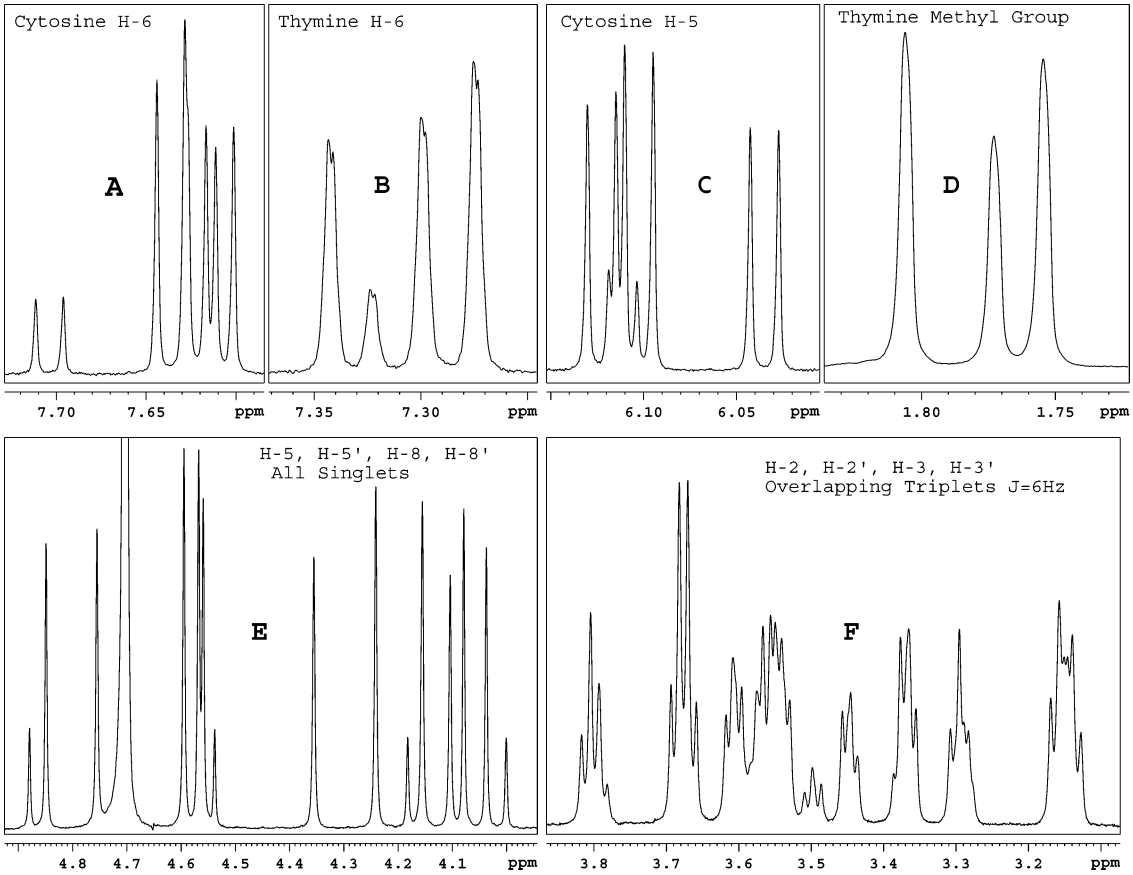

Figure 6. ^{1}H NMR spectrum of the (CT) PNA dimer in D_2O at 500 MHz.

Table 1. ^{1}H NMR Assignments of (CT) PNA Dimer (500.13 MHz − D_2O)[a]

H	A	B	C	D	H	A	B	C	D
2	3.29 t	3.16 t	3.30 t	3.14 t	2′	3.38 t	3.37 t	3.45 t	3.43 t
3	3.80 s	3.68 s	3.81 s	3.67 s	3′	3.50 t	3.61 t	3.54 t	3.56 t
5	4.00 s	5.16 s	4.11 s	4.35 s	5′	4.18 s	4.24 s	4.04 s	4.08 s
8	4.88 s	4.60 s	4.85 s	4.56 s	8′	4.54 s	4.57 s	4.71 s	4.76 s
C-H5	6.11 d	6.11 d	6.04 d	6.12 d	T-H6	7.32 bq	7.27 bq	7.34 bq	7.30 bq
C-H6	7.70 d	7.64 d	7.62 d	7.61 d	T-CH_3	1.80 d	1.76 d	1.77 d	1.81 d

[a] $J_{2,3}$ and $J_{2'}$,3′ ≈ 6 Hz; $J_{C-H5,C-H6}$ = 8 Hz; $J_{T-H6,T-CH3}$ = 1 Hz; bq = broad quartet.

NOESY spectrum was used to observe the NOE cross-correlation peaks between H-8 and H-3 or H-8′ and H-3′ if the carbonyl C-7 were to be pointing toward the C terminus, or NOE cross-correlation peaks between H-8 and H-5 or H-8′ and H-5′ if the C-7 carbonyl group were to be pointing toward the N terminus. The full assignments for all four (CT) PNA rotamers are tabulated in Table 1. In the ^{1}H NMR spectrum, all the signals corresponding to the methylene protons H-5, H-8, H-5′, and H-8′ appeared as singlets (Figure 6, inset E), and all the signals corresponding to the methylene protons H-2, H-3, H-2′, and H-3′ appeared as triplets with a coupling constant $J_{2-3} \approx 6$ Hz (Figure 6, inset F). The degeneracy in chemical shift of each pair of protons of the methylene groups clearly indicates that the structure of the single-stranded (CT) PNA dimer is random coil. Only free rotation around all the bonds can produce singlets for the isolated methylene groups (H-5, H-8, H-5′, H-8′) and triplets with average vicinal coupling constant of ∼6 Hz for the vicinal methylene groups (H-2, H-3, H-2′, H-3′). The degeneracy on the chemical shift of the methylene protons was also observed in the one-bond proton−carbon heteronuclear correlations in the ^{1}H,^{13}C HSQC experiments (not shown). Only one signal per CH_2 protons correlates with its corresponding carbon signal.

Scheme 4. Newman Projection of a Right-Handed and Left-Handed Helical (CT) PNA

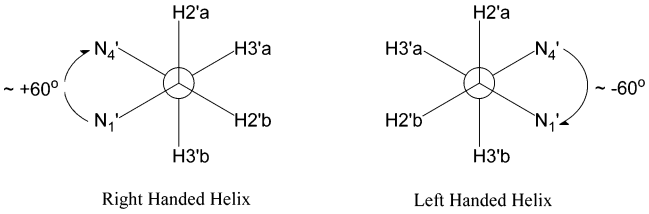

Consistent with the X-ray crystal structure of PNA−DNA,[40] the NMR solution structure of PNA−RNA,[41] and computer models of (CT) PNA dimer generated in our group, the torsion angle formed by N1′-C2′-C3′-N4′ should adopt values in the range of +50° to +60° for the structure to form a right-handed

(40) Brown, S. C.; Thomson, S. A.; Veal, J. M.; Davis, D. G. *Science* **1994**, *265*, 777−780.
(41) Menchise, V.; De Simone, G.; Tedeschi, T.; Corradini, R.; Sforza, S.; Marchelli, R.; Capasso, D.; Saviano, M.; Pedone, C. *Proc. Natl. Acad. Sci. U.S.A.* **2003**, *100*, 12021−12026.

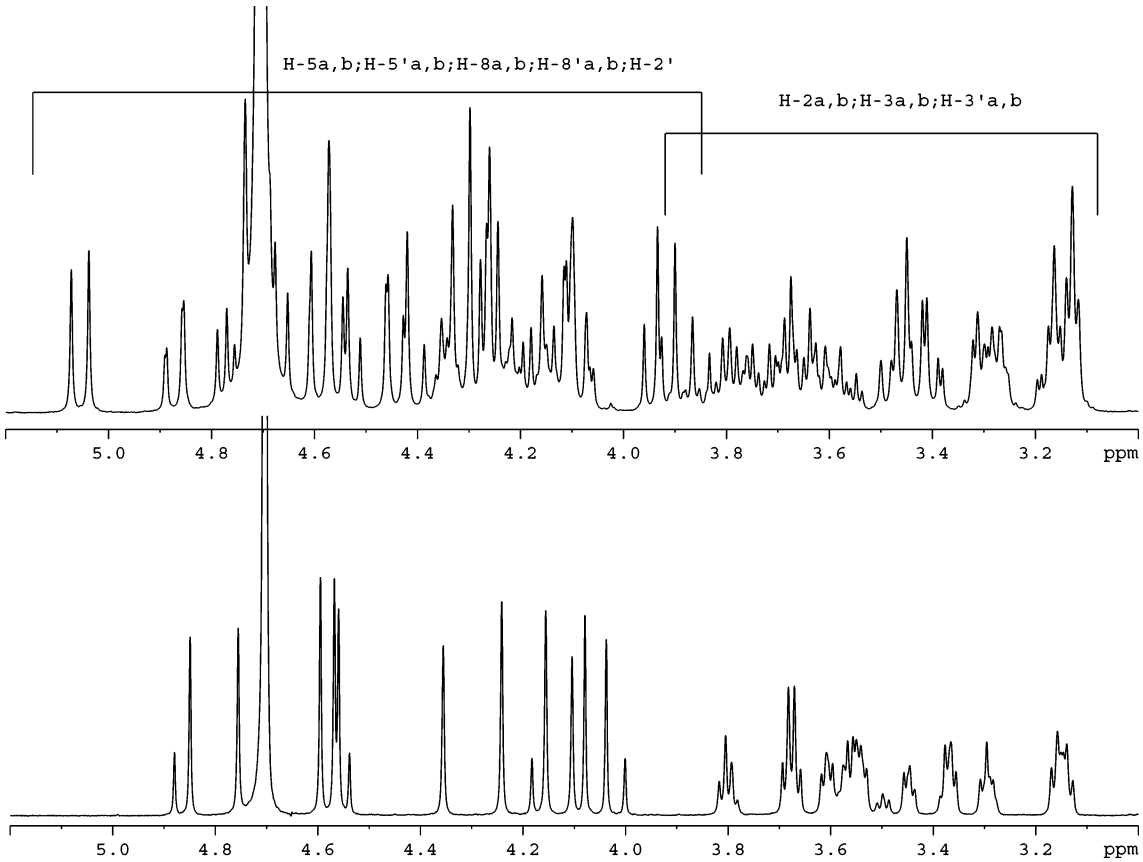

Figure 7. ^{1}H NMR spectrum of (C^L**T**) ^{L}Ala-γPNA (top trace) and PNA (bottom trace) in D_2O at 500 MHz. Expansion of the backbone CH_2 proton signals.

Scheme 5. Chemical Structures of the Four (C^{L}T) ^{L}Ala-$^\gamma$PNA Rotamers

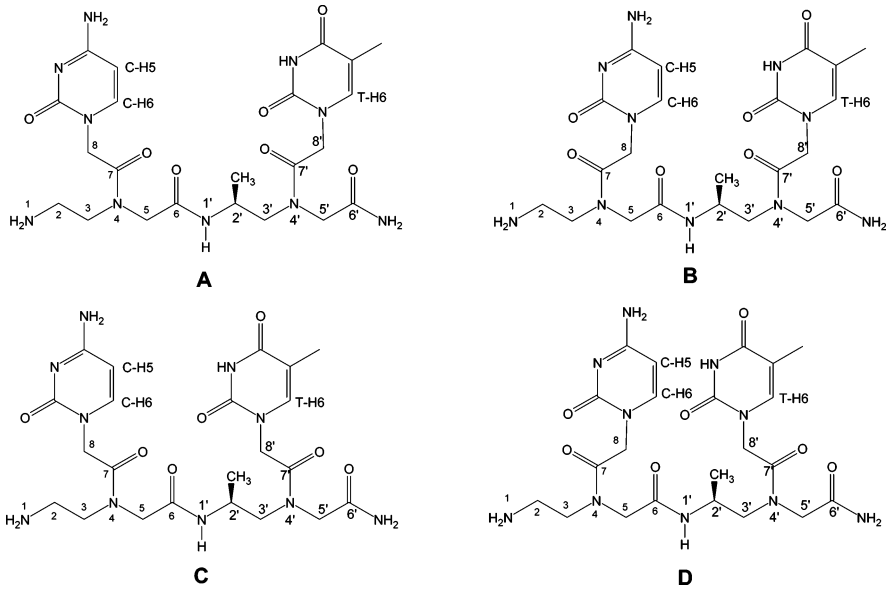

helix. An opposite sign of the dihedral angle is needed to form a left-handed helix, Scheme 4. Although PNA is achiral, once both the right-handed and left-handed helical structures are formed, they are mirror images of one another, and the NMR signals should be the same for both.

If both the right-handed and left-handed helices were to be present in solution, the signals corresponding to H-2′ and H-3′ should not appear as simple triplets with J couplings of ∼6 Hz. Each proton at each CH_2 should not be chemically equivalent. Instead, the NMR spectrum should show four complex multiplets for H-2′a, H-2′b, H-3′a and H-3′b. On the basis of the dihedral angles involving these protons and a rough estimation of J values using the Karplus equation, the NMR spectrum should show two doublets of doublet of doublet (ddd) of 14, 10, and 3 Hz for a right-handed helix, and two doublets of doublet of doublet (ddd) of 14, 3, and 3 Hz for a left-handed helix—where the 14 Hz corresponds to the geminal coupling constant, 10 Hz to the trans diaxial vicinal coupling constant, and 3 Hz for a coupling constant for a torsion angle of ∼+60°. These signals, however, were not observed—ruling out the possi-

Table 2. ^{1}H NMR Assignments of (C^{L}T) ^{L}Ala-γPNA (500.13 MHz − D_2O)[a]

H	A	B	C	D	H	A	B	C	D
2	3.30 t	3.16 t	3.27 t	3.13 t	3′a	3.61 dd	3.70 dd	3.49 dd	3.48 dd
3a	3.88 m	3.77 m	3.81 m	3.69 m	3′b	3.18 dd	3.30 dd	3.45 dd	3.40 dd
3b	3.74 m	3.56 m	3.79 m	3.62 m	5′a	4.20 d	4.27 d	4.28 d	4.26 d
5a	4.13 d	4.18 d	3.85 d	4.44 d	5′b	4.08 d	4.27 d	3.94 d	3.92 d
5b	4.08 d	4.09 d	4.09 d	4.28 d	8′a	4.59 d	4.67 d	4.73 d	5.06 d
8a	4.87 d	4.69 d	4.87 d	4.59 d	8′b	4.37 d	4.44 d	4.73 d	4.55 d
8b	4.77 d	4.53 d	4.75 d	4.32 d	T-H6	7.32 bq	7.28 bq	7.33 bq	7.29 bq
C-H5	6.01 d	6.05 d	6.03 d	6.06 d	T-CH_3	1.79 bd	1.77 bd	1.79 bd	1.80 bd
C-H6	7.62 d	7.57 d	7.59 d	7.51 d	Ala CH_3	1.09 d	1.16 d	1.18 d	1.20 d
2′	4.21 m	4.15 m	4.22 m	4.34 m					

[a] $J_{2,3} \approx 6$ Hz; $J_{5a,5b} = J_5'a,5'b = J_{8a,8b} = J_8'a,8'b \approx 17$ Hz; J_2', AlaCH3 = 6.7 Hz; J_2',3′a = 10.2 Hz; J_2',3′b = 4.2 Hz; J_3'a,3′b = 15.2 Hz; $J_{C-H5,C-H6} = 8$ Hz; $J_{T-H6,T-CH3} = 1$ Hz; bd = broad doublet; bq = broad quartet.

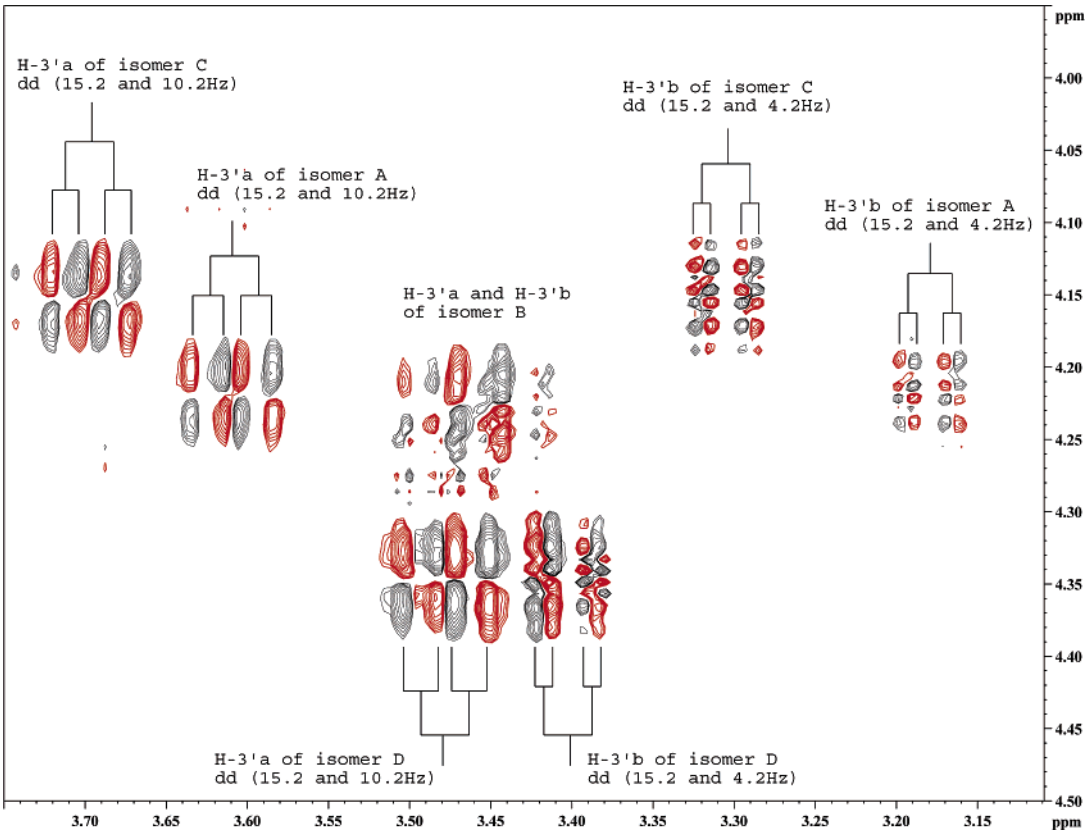

Figure 8. Double-quantum-filtered-phase-sensitive COSY of (C^L**T**) ^{L}Ala-γPNA in D_2O at 500 MHz.

bility that these dimers existed in an equal population of right-handed and left-handed helices.

Solution Structure of (C^{L}T) ^{L}Ala-γPNA Dimer. The ^{1}H NMR spectrum of the ^{L}Ala-γPNA dimer, on the other hand, showed an entirely different set of signals (Figure 7, top trace). The structures of the four rotamers are shown in Scheme 5 and the ^{1}H NMR assignments in Table 2. The degeneracy in chemical shift is broken for all of the methylene groups except for H-2, which freely rotates at the N terminus and produced a triplet with an average coupling constant of ∼6 Hz (signals at 3.1−3.2 ppm in Figure 7, top trace). Figure 7 clearly shows the differences between the ^{1}H NMR spectra of ^{L}Ala-γPNA and PNA (Figure 7, top and bottom trace, respectively). Similar to that of the PNA dimer, the ^{1}H NMR spectrum of the ^{L}Ala-γPNA dimer showed signals corresponding to the four rotamers in solution (Figure 7, top trace). The spectrum of ^{L}Ala-γPNA, however, is more complex. The methylene protons H-5, H-8, H-5′, and H-8′ no longer appeared as singlets. Each methylene proton is no longer chemically equivalent, and they appeared as 17 Hz doublets (geminal coupling constant). The most interesting part of the ^{1}H NMR spectrum is the signals displayed by the spin system composed of H-2′, H-3′a, H-3′b, and the CH_3 group attached to C-2′. Due to the significant signal overlapping in the 1D ^{1}H NMR spectrum, a double-quantum-filtered-phase sensitive COSY experiment was performed to resolve and identify the coupling pattern of this spin system. Four sets of signals were observed due to the presence of four rotamers, Figure 8. Proton H-2′ appeared as a complex multiplet due to coupling to the CH_3 and to protons H-3′a and H-3′b. The signal of H-3′a appeared as doublet of doublet with coupling constants of 15.2 and 10.2 Hz, while H-3′b appeared as a doublet of doublet with coupling constants of 15.2 and 4.2 Hz (Figure 9, top left trace). This indicates that the presence of a preferred conformation in solution that involves one trans diaxial inter-

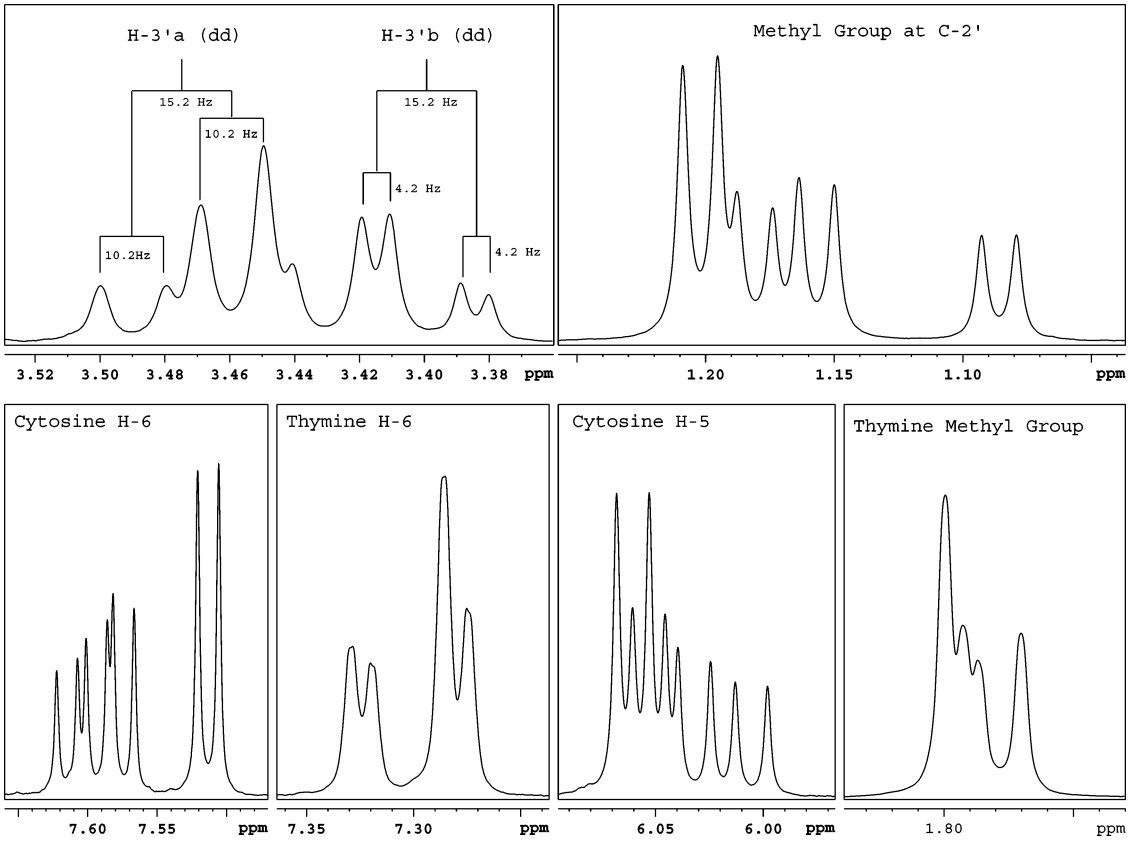

Figure 9. ^{1}H NMR spectrum of (CT) ^{L}Ala-γPNA in D_2O at 500 MHz. Base aromatic signals. (Top left) H-3′a and H-3′b signals of the major rotameric isomer. (Top right trace) signals (doublets) of the CH_3 group at C-2′.

Scheme 6. Newman Projection of a Right-Handed and Left-Handed (C^{L}T) ^{L}Ala-γPNA

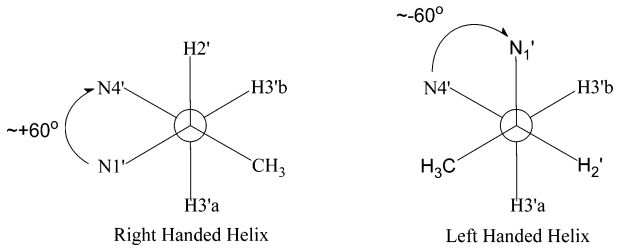

action between H-2′ and H-3′a (J of 10.2 Hz) (Scheme 6, left structure) and an axial to equatorial interaction between H-2′ and H-3′b (J of 4.2 Hz). Given that the absolute configuration at C-2′ is S, the only conformation that produces this relative spatial arrangement of protons H-2′, H-3′a, and H-3′b is the one that leads to the formation of a right-handed helix. No evidence for the formation of a left-handed helix was observed in the NMR spectrum. If a left-handed helix were to be present in solution, the coupling pattern of H3′a and H3′b would be the same. Both should show a small vicinal coupling constant of ~4 Hz leading to a doublet of doublet of ~15 and 4 Hz for both protons. Furthermore, the spectrum should also show methyl signals for a left-handed helical conformation. In this case, a total of eight methyl signals should appear in the 1D ^{1}H NMR spectrum; however, only four methyl signals were observed (Figure 9, top right trace).

The helical sense of γPNAs, in this case, is determined by the stereochemistry at the γ-position (C-2′). The S configuration prefers a right-handed helix because the amino acid side chain, in this case the CH_3 group, prefers a trans diaxial relationship with N4′ to minimize steric clash. In a left-handed helical conformation the gauche interaction between CH_3 and N4′ increases the energy of the system. AM1 semiempirical calculations of the (C^L**T**) ^{L}Ala-γPNA dimer in both the left- and right-handed conformations showed a difference in the heat of formation of 3.5 kcal/mol in favor of the right-handed helix. Assuming a zero change in entropy between the two conformations, the ΔH is equal to the ΔG. With a $\Delta\Delta G$ of 3.5 kcal/mol, more than 99% of the dimer should be in the right-handed helical conformation.

The NMR data indicate that the four rotamers of (C^L**T**) ^{L}Ala-γPNA are in a right-handed helical conformation. The solution structure of ^{L}Ala-γPNA obtained from NMR analysis is surprisingly similar to that of the unmodified PNA in a PNA−DNA hybrid duplex, as determined by X-ray crystallography (compare the two structures in Figure 10).[41] (Note the similarity in the backbone conformation.) These NMR results provide strong evidence for the existence of γPNA exclusively in a right-handed helical conformation—resembling that of PNA in PNA−DNA and PNA−RNA double helix. On the basis of these results we can anticipate that any substitution at C-2′ (γ-position) will lead to a preferred, helical preorganization of the backbone—the helical sense of which will be determined by the stereochemistry at this position. The S configuration will prefer a right-handed helix, while the R configuration will prefer a left-handed helix. The substituent C-2′ appears to be the determining factor that directs the helical folding of γPNAs. We suggest that helical induction occurs as the result of steric clash in the backbone, between substituent at the C-2′ (γ-position) and N4′, followed

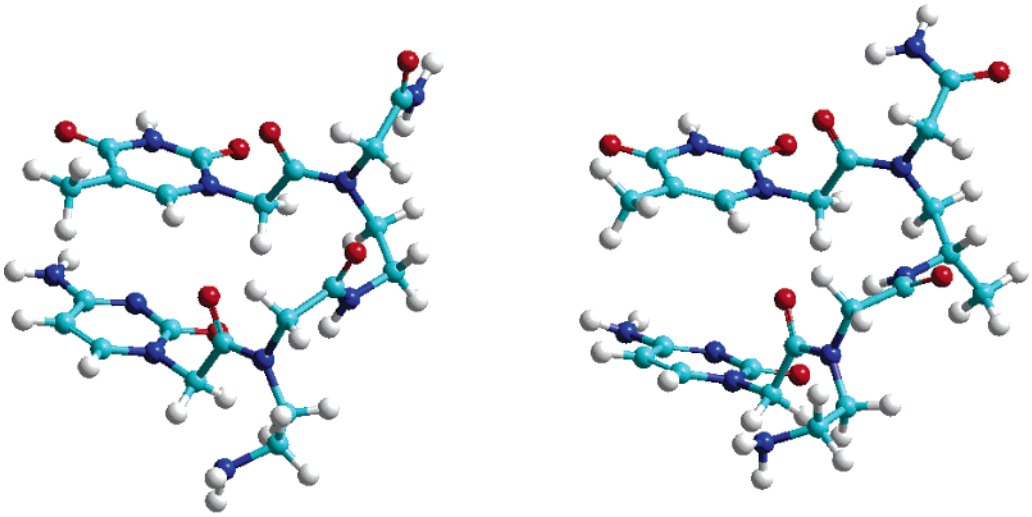

Figure 10. (A) X-ray structure of PNA in a PNA−DNA duplex[41] and (B) solution structure of (C^{L}**T**) ^{L}Ala-γPNA determined by NMR.

Table 3. Melting Transitions (T_m's)[a] of Hybrid Duplexes

PNA	sequence	T_m (°C)	ΔT_m (°C)
P1	H-GCATGTTTGA-^{L}Lys-NH_2	(44) 54	
P2	H-GCATG$^{\gamma}$**T**TTGA-^{L}Lys-NH_2	(48) 57	(+4) +3
P3	H-GCA$^{\gamma}$**T**G$^{\gamma}$**T**T$^{\gamma}$**T**GA-^{L}Lys-NH_2	(53) 60	(+9) +6
P4	H-GCATG$^{\gamma}$**T**$^{\gamma}$**T**$^{\gamma}$**T**GA-^{L}Lys-NH_2	(53) 59	(+9) +5
P5	H-$^{\gamma}$**G**$^{\gamma}$**C**$^{\gamma}$**A**$^{\gamma}$**T**$^{\gamma}$**G**$^{\gamma}$**T**$^{\gamma}$**T**$^{\gamma}$**T**$^{\gamma}$**G**$^{\gamma}$**A**-^{L}Lys-NH_2	(63) 64	(+19) +10

[a] T_m's of PNA−DNA (in parentheses) and PNA−RNA hybrid duplexes in sodium phosphate buffer at 2 μM strand concentration each.

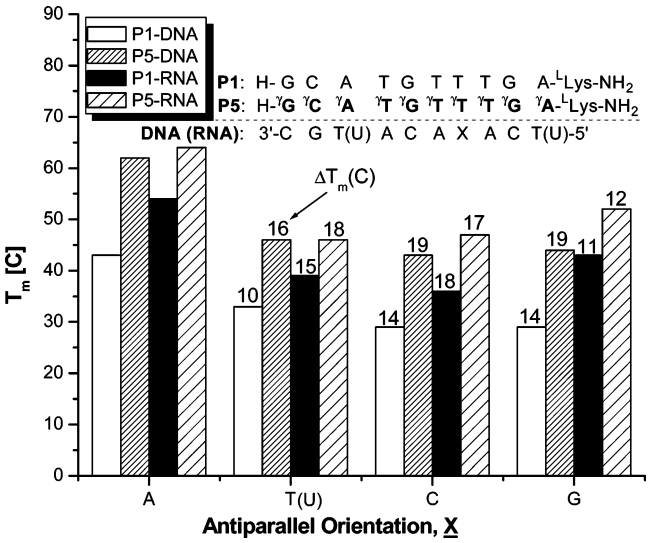

Figure 11. T_m's of P1−DNA, P5−DNA, P1−RNA and P5−RNA hybrid duplexes containing perfectly matched and single-base mismatched sequences, where X = A, C, G, T(U).

by base-stacking—which provides the added stability to the structure. This is clearly observed in the computer-generated structures.

The Effects of Structural Preorganization on the Binding Affinity and Sequence-Specificity of PNA. To determine whether structural preorganization contributes to the hybridization stability of PNA, we measured the melting transitions (T_m's) of the various ^{L}S-γPNAs (P2−P5) with complementary DNA and RNA strands and compared them to that of PNA (P1), Table 3 (and Figures S5 and S6, Supporting Information). On average, the T_m's of the hybrid duplexes increased by ∼3 °C for DNA and ∼2 °C for RNA for every chiral unit incorporated. The hybridization stability, in this case, is not affected by backbone spacing as compared to the modification made at the α-position (compare the T_m of P3 to that of P4).[24] The extent of this stabilization is significant, considering that no charge−charge interaction is involved and that the modified unit can be incorporated at every position without compromising the overall binding affinity, unlike the observations made with α-PNAs.[24] In addition to the high binding affinity, these modified ^{L}S-γPNAs bind to DNA and RNA with high sequence selectivity, Figure 11 (and Figures S7 and S8: Supporting Information). A single-base mismatch lowered the T_m by 16−19 °C for DNA and 12−18 °C for RNA, depending on the mismatched pair, as compared to 10−14 °C and 11−18 °C, respectively, for PNA (P1).[32] This improvement could be attributed to structural preorganization.

Conclusion

In summary, we have shown that a simple γ-backbone modification can transform a randomly folded PNA into a right-handed helical structure. These helical PNAs bind to DNA and RNA with exceptionally high affinity and sequence selectivity. Helical induction, in this case, occurs in the C- to N-terminal direction. The determining factor for helical induction appears to be sterically driven, and stabilized by base-stacking. This finding suggests that it may be possible to assemble other chromophores into organized arrays. The results reported herein have important ramification not only on the future design of nucleic acid mimics with high binding affinity and sequence-selectivity but also for the design of novel materials with more precise spatial organization and efficient electronic coupling[42−46]—for possible applications in molecular electronics and photonic devices.

(42) Arai, T.; Inudo, M.; Ishimatsu, T.; Akamatsu, C.; Tokusaki, Y.; Sasaki, T.; Nishino, N. *J. Org. Chem.* **2003**, *68*, 5540−5549.
(43) Solladie, N.; Hamel, A.; Gross, M. *Tetrahedron Lett.* **2000**, *41*, 6075−6078.
(44) Dunetz, J. R.; Sandstrom, C.; Young, E. R.; Baker, P.; Van Name, S. A.; Cathopolous, T.; Fairman, R.; de Paula, J. C.; Akerfeldt, K. S. *Org. Lett.* **2005**, *7*, 2559−2561.
(45) Hippius, C.; Schlosser, F.; Vysotsky, M. O.; Bohmer, V.; Wurthner, F. *J. Am. Chem. Soc.* **2006**, *128*, 3870−3871.
(46) van der Boom, T.; Hayes, R. T.; Zhao, Y.; Bushard, P. J.; Weiss, E. A.; Wasielewski, M. R. *J. Am. Chem. Soc.* **2002**, *124*, 9582−9590.

Acknowledgment. We are grateful to Carnegie Mellon University and the Department of Chemistry for financial support. The NMR spectrometers in the Department of Chemistry NMR Facility at Carnegie Mellon University were purchased in part with funds from the National Science Foundation (CHE-0130903).

Supporting Information Available: Synthesis of ^{L}S-γPNA monomers and oligomers, HPLC and MALDI-TOF traces of P5, CD spectra of other L-serine derived PNA oligomers, double-quantum-filtered-phase-sensitive COSY of (C^{L}**T**) ^{L}Ser-γPNA in D_2O at 500 MHz, UV-melting curves of PNA−DNA and PNA−RNA hybrid duplexes containing perfectly matched and single-base mismatched sequences, and CD spectra of PNA oligomers containing different nucleobase sequence at the adjacent N-terminal position with respect to the chiral backbone units. This material is available free of charge via the Internet at http://pubs.acs.org.

JA0625576